

# Experimental and Simulation Study of Tensile Strength of Banana and Glass Fibres and their Hybrid Epoxy Composites

Mustafa Nordin<sup>1</sup>, Mohd Rozaiman Aziz<sup>1,\*</sup>, Rozaini Othman<sup>1</sup>

<sup>1</sup>Faculty of Mechanical Engineering, Universiti Teknologi MARA Cawangan Pulau Pinang, 13500 Permatang Pauh, Pulau Pinang, Malaysia. \*corresponding Author: man@uitm.edu.my

# **ABSTRACT**

In recent years, the growing emphasis on sustainability has driven researchers to explore eco-friendly materials that can provide sufficient mechanical strength while minimizing environmental impact. Composite materials have gained prominence for their ability to combine the advantageous properties of different constituents. In particular, hybrid composites composed of multiple fibre types offer potential for use in demanding industries such as aerospace and automotive manufacturing. Although fibreglass and epoxy are widely recognized for their excellent mechanical performance, the integration of natural fibres such as banana fibre in hybrid composites remains limited. Previous studies have also revealed a notable lack of simulation-based research focusing on banana fibre reinforcement, whether as a standalone material or in combination with fibreglass. Therefore, this gap highlights the need to further investigate and validate the mechanical performance of banana-glass fibre composites through both experimental and simulation approaches. This study aims to determine the optimal tensile properties of glass fibre and banana fibre composites with various layer configurations and validate the simulation results against experimental findings to ensure the accuracy and reliability of the modelling approach. The composites were fabricated using the hand lay-up method and evaluated through tensile testing and simulation. The findings showed that the L1 configuration, composed entirely of glass fibre, exhibited the highest tensile strength, recording an ultimate load of 5.96 kN and an ultimate stress of 119.46 MPa experimentally, while simulation results yielded 5.83 kN and 119.06 MPa. In contrast, the L2 configuration, made solely of banana fibre, showed the lowest tensile performance, with an ultimate load of 1.13 kN and ultimate stress of 10.17 MPa experimentally, compared to 1.11 kN and 9.84 MPa in simulation. Among the hybrid laminates, L4 (5 glass fibre layers and 4 banana fibre layers) outperformed L3 (4 glass fibre layers and 5 banana fibre layers), attributed to its layer arrangement that enhanced structural integrity. The percentage error between experimental and simulated results was below 4%, confirming strong correlation and model accuracy. Both research objectives were successfully achieved. The results demonstrated that glass fibre significantly enhances the tensile strength of hybrid composites, while banana fibre contributes to environmental sustainability with moderate strength retention. Overall, the study validates the feasibility of using banana-glass fibre hybrid composites and supports their potential application in lightweight, sustainable engineering materials. The first objective, which aimed to determine the optimal tensile properties of glass fibre and banana fibre in various configurations by adjusting their layer arrangements, was successfully achieved. The second objective, focused on validating the tensile properties obtained from simulation results against experimental findings, was also successfully fulfilled where the percentage error was below percentage error of 4%. The results indicate that the laminate composed entirely of glass fibre layers (L1) exhibited the highest tensile properties, whereas the laminate consisting solely of banana fibre layers (L2) demonstrated the lowest tensile strength. In the case of hybrid composites, glass fibre contributed a significantly greater effect on the overall strength compared to banana fibre alone. Among the hybrid laminates, L4 achieved higher ultimate load and ultimate stress than L3, which could be attributed to its lay-up configuration where two glass fibre layers were positioned between two banana fibre layers, thereby enhancing the structural integrity of the composite.

Keywords: Composite; tensile properties; banana fibre; glass fibre; epoxy

# Nomenclature (Greek symbols towards the end)

$ ho_{gf}$	Density Glass Fibre (g/cm³)
$W_{gf}$	Weight of Glass Fibre (g)
$ ho_{bf}$	Density of Banana Fibre (g/cm <sup>3</sup> )
$W_{bf}$	Weight of Banana Fibre (g)
$ ho_m$	Density of Matrix (g/cm <sup>3</sup> )
$W_{mgf}$	Weight of matrix for glass fibre (g)
$W_{mbf}$	Weight of matrix for banana fibre (g)

Received on 26.07.2025 Accepted on 22.10.2025 Published on 07.11.2025

$E_{11}$	Axial stiffness of the composite (MPa)
$E_{22}$	Transverse stiffness of the composite (MPa)
$V_{12}$	Poison's ratio of the composite
$G_{12}$	Axial shear stiffness (MPa)
$G_{23}$	Shear stiffness (stress) acting in the 1 direction on a plane with a normal in the 3 direction (MPa)
$G_{31}$	Shear stiffness (stress) acting in the 2 direction on a plane with a normal in the 3 direction (MPa)
$X_T$	Longitudinal tensile strength (MPa)
$X_{C}$	Longitudinal compressive strength (MPa)
$Y_T$	Transverse tensile strength (MPa)
$Y_{C}$	Transverse compressive strength (MPa)
$S_L$	Longitudinal shear strength (MPa)
$S_T$	Transverse shear strength (MPa)
$G_{XT}$	Longitudinal tensile fracture energy (N/mm)
$G_{XC}$	Longitudinal compressive fracture energy (N/mm)
$G_{YT}$	Transverse tensile fracture energy (N/mm)
$G_{YT}$	Transverse compressive fracture energy (N/mm)

#### **Abbreviations**

LI	Laminate 1
L2	Laminate 2
L3	Laminate 3
L4	Laminate 4
$\mathrm{B}_{\mathrm{F}}$	Banana Fibre
$G_{F}$	Glass Fibre
$V_{\rm f}$	Volume Fibre
$V_{m}$	Volume matrix
$V_{GF}$	Volume Glass Fibre
$V_{BF}$	Volume Banana Fibre

#### 1.0 INTRODUCTION

In the realm of composite materials, a diverse group of researchers has contributed to the study of mechanical properties such as tensile properties and flexure modulus of natural and synthetic fibres reinforced polymer composites [1][2]. The natural fibres such as banana used in composite materials have an advantage due to its eco-friendly waste and low impact to the environment properties. Hence, it is suitable in the development of biodegradable and renewable composite materials. It was also recommended to serve as an alternative to a synthetic fibre such as glass fibre [3][4]. For example, hemp and banana fibres produced comparable performance to synthetic fibres in helmet manufacturing [5]. Nonetheless, a study showed that glass fibre composites exhibited higher tensile strength and fracture toughness compared to banana fibre composites [3]

To further improve the performance of banana fibre reinforced composites, hybridization process was introduced. The finding suggested the potential of these composites for diverse applications, offering enhanced stiffness, elasticity, and ultimate tensile strength [6]. Prabhu et al. investigated the mechanical properties of flax, banana, and industrial waste tea leaf fibre-reinforced hybrid polymer composites, highlighting the superior mechanical characteristics of specific fibre combinations [7]. Similarly, Reddy et al. explored the influence of glass fibre on the mechanical properties of banana fibre-reinforced epoxy composites, emphasizing the significant impact of glass fibre on various mechanical properties [8]. Karthick et al. evaluated the mechanical behaviour of banana fibre-reinforced hybrid epoxy composites, indicating the significant effect of fibre length and loading contribution in composite materials [9]. The hybridization of E-glass and banana fibres also yielded a better water absorption and flexural properties of epoxy composites [10]. Rouf et al. explored the use of alkali-treated banana fibres as natural reinforcement in gypsum and resulted in improvement of interfacial bonding.

Apart from hybridization of composites, the mechanical properties of composite materials are enhanced by incorporating particle such as nano marble dust particles in banana/sisal fibre composites and rice husk fillers at specific fibre volume fractions banana/epoxy composites. It helps in enhancing their flexural strength, impact resistance, and thermal conductivity [11] [12]. Likewise, the treated banana fibre improves the mechanical properties compared to the untreated one. These findings indicate the potential of these composites for various industrial applications, offering a cost-effective and sustainable alternative to traditional materials [13].

Furthermore, studies conducted by Santhanam et al. [14], Batu and Lemu [15] and Negawo et al. [16] revealed the effects of fibre orientation, volume fraction and hybridization to enhance mechanical properties of banana/glass fibre reinforced composites. Based on the results, it was suggested the hybrid banana/glass could be a potential application for load-bearing structures. In a study conducted by Omprakasam et al. [17], banana fibre with madar fibre composites provides a feasible and sustainable replacement to conventional PCBs.

Koloor et al. [18] investigated composite structures composed of multidirectional (MD) fibre-reinforced polymer (FRP) laminates, which typically fail through various damage mechanisms in the matrix, interface, and fibres at different scales. In their approach, the composite was modelled using the lamina strength limit to represent the onset of damage. However, the yielding behaviour of MD composites in structural applications remains difficult to quantify because of the complex sequence of damage progression across laminas, which depends on their orientation and properties. To address this, the study introduced a new method for identifying the yield point of MD composite structures by analysing the evolution of damage dissipation energy (DDE). Through a simulation study, the yield points of three antisymmetric MD FRP composite structures under flexural loading were established and compared using both the Hashin unidirectional (UD) failure criteria and the energy-based criterion.

Al Rashid et al. [19] explored the development of new materials for field hockey equipment with the aim of reducing manufacturing costs and minimizing the environmental impact associated with synthetic materials, while maintaining the quality and performance of the final product. Their review of natural fibres highlighted their excellent mechanical properties and strong compatibility for composite applications. In their study, simulation models were developed using ABAQUS, replicating the specimen geometry used in experimental tests. The supports and rollers were modelled as rigid, non-deformable materials to simplify boundary conditions. Subsequently, the composite laminates were constructed symmetrically, and the material properties were defined using engineering constants to represent the lamina characteristics accurately.

Based on the literatures, these studies have collectively contributed to the understanding of the mechanical properties and potential applications of natural and synthetic fibre composites, as well as the effects of specific materials on composite properties. The research findings underscored the importance of material selection, hybridization, and treatment in optimizing the performance of composite materials for various applications. These insights have significant implications for industries such as automotive, construction, aerospace, and more, where lightweight, strong, and environmentally friendly materials are in high demand. Nevertheless, the previous investigations were based on experimental testing. In order to further evaluate the mechanical behaviour and characteristics of banana and glass fibre reinforced epoxy, numerical simulation can be utilized as a research method. Hence, this study focuses to examine the effects of varying volumes of banana and glass fibres in epoxy composites to the tensile strength via both experiment and numerical simulation.

# 2.0 METHODOLOGY

The methodology of this study, as illustrated in **Figure 1**, outlines the process flow sequence that incorporated both experimental and simulation approaches. The experimental work began with the preparation of materials, namely banana fibre, glass fibre, resin, and hardener. Specimens with different laminate configurations were fabricated using the hand layup technique. These specimens were then subjected to tensile testing to determine the optimal tensile properties for various configurations of glass fibre and banana fibre.

For the simulation, Abaqus software was employed. The procedure consisted of seven steps: designing the specimen, assigning material properties, defining the analysis step, applying loads, generating the mesh, running the simulation, and finally, obtaining the results. Convergence analysis was also conducted to determine the optimal mesh size.

Finally, the experimental and simulation results were compared to validate the tensile properties obtained from simulation against those from experimentation, confirming the determination of the optimal tensile properties for the studied laminate configurations.

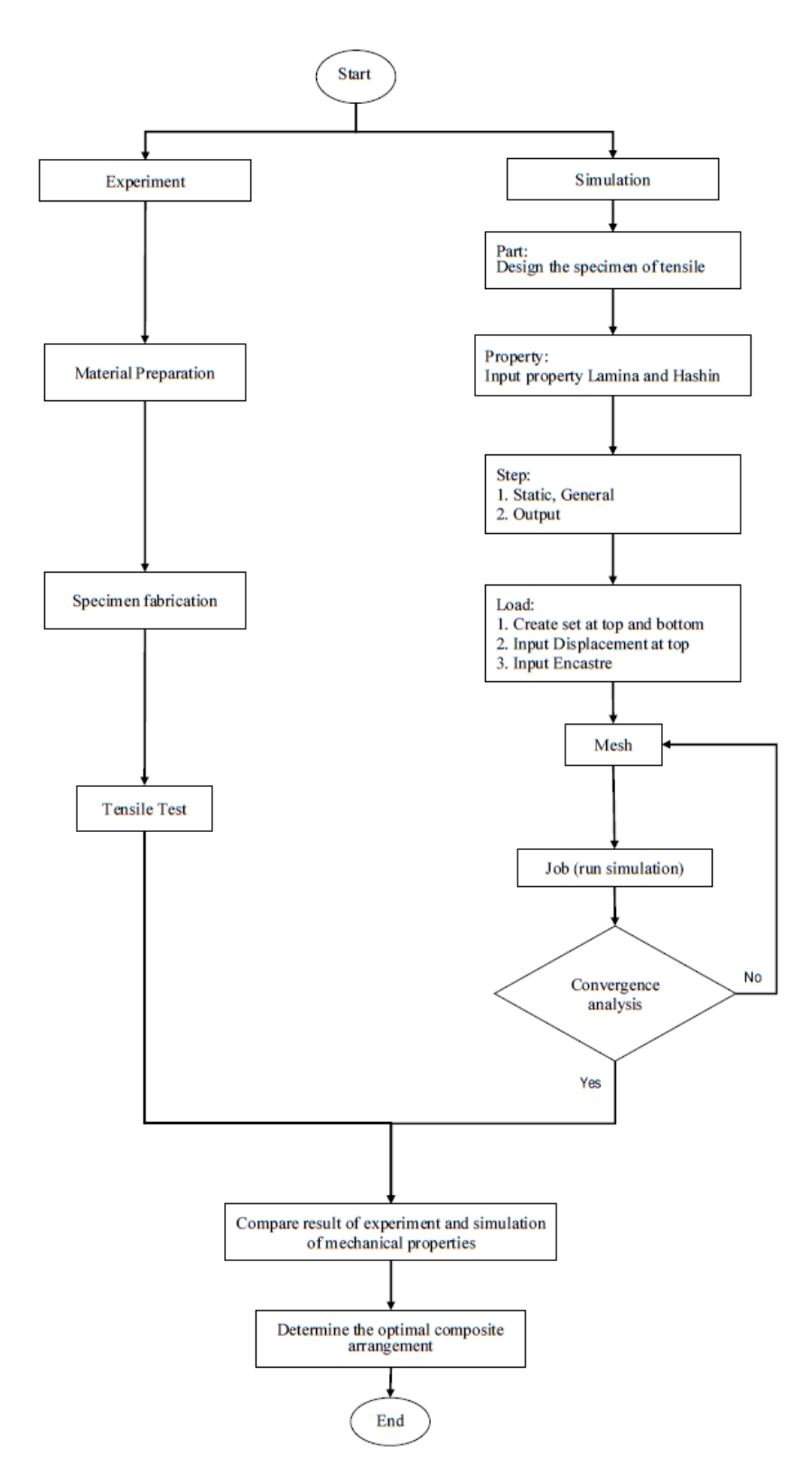


Figure 1. Flow chart of study

#### 2.1 Experiment setup

The preparation began with the selection of glass fibre in the form of woven roving. As illustrated in **Figure 2** (a), woven roving consisted of continuous rovings woven into a fabric and was commonly used for manufacturing flat laminates. This reinforcement allows the integration of higher-quality fibres into the composite, thereby enhancing its specific strength. Glass fibre was chosen as the reinforcement material due to its easy availability, high stiffness, flexibility in fibre placement, and cost-effectiveness[20].

Banana fibre was sourced from Indonesia, as illustrated in **Figure 2**(b). The extraction process involved squeezing the banana plant's stem, which resembles a trunk, to remove approximately 60% of its water and lignin. The stem was then submerged in stagnant water for 10 to 15 days to dissolve the remaining lignin, after which it was washed with clean water and dried in open air at room temperature [21]. The raw banana fibres were subsequently treated with sodium hydroxide (NaOH) to remove wax, hemicellulose, and residual lignin from the fibre surface, as shown in **Figure 3**, and were then sun-dried.

The hand lay-up process began with the preparation of the matrix by mixing epoxy resin and hardener in a 10:1 ratio. Wax was applied to the board to act as a releasing agent (**Figure 4**). Using the hand lay-up technique (**Figure 5**), nine (9) plies of fibre were fabricated [21] [20]. Epoxy resin was poured and uniformly spread with a roller, which also assisted in removing trapped air and enhancing bonding with the gel coat. Each ply was placed sequentially with resin application until all nine plies were laminated. The laminates were then cured at room temperature for 24 hours, during which a load of approximately 20 kg was applied to each composite cast to ensure proper consolidation and solidification [22].

Four types of specimens were fabricated and tested, consisting of nine plies of glass fibres, nine plies of banana fibres, four plies of glass fibres with five plies of banana fibres, and four plies of banana fibres with five plies of glass fibres. The specimens were cut according to the ASTM D638 standard [23], as shown in **Figure 6**. This standard was chosen because it specifies the procedure for determining the tensile properties of specimens under defined conditions of pretreatment, temperature, humidity, and testing machine speed. The thickness of the specimens in this study ranged from 5.1 mm to 13.5 mm, and the crosshead speed during testing was set at 1 mm/min.[23]

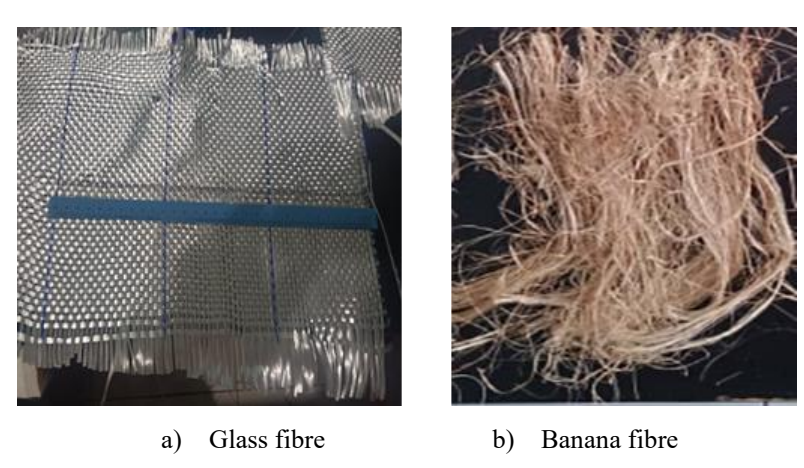


Figure 2: Raw materials as reinforcement fibre used in the study



Figure 3: Treat banana fibre with NaoH





Figure 4. Wax applied on the board



Figure 5. Hand lay-up process

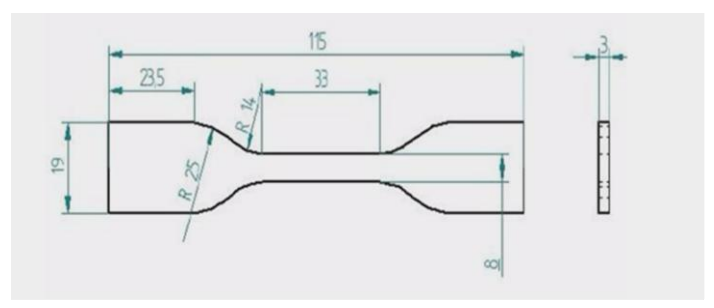


Figure 6. Tensile test specimen

## 2.2 Simulation

Subsequently, simulations were conducted using ABAQUS software, and the results from both the experimental and simulation phases were compared for analysis. The process began by developing a 3D model of the tensile test specimen, adhering to the dimensions and geometry presented in Figure 7. Material properties, including the Lamina property (Figure 8) and Hashin's failure criteria (Figure 9) [24] were then assigned to the model. To enhance the accuracy of the simulation, data sets were imported from reliable sources such as Monzón et al. [25] and Koloor et al. [18]. By carefully importing and defining these data sets, the simulation was able to replicate real-world behaviour more effectively, resulting in reliable and valid outcomes. This preparation is a crucial stage in the process, as it establishes the foundation for generating a realistic and precise simulation, ensuring that the final model accurately represents the intended design and operational conditions.

It was further assumed that both glass fibre epoxy and banana fibre epoxy materials exhibited anisotropic and orthotropic characteristics [26]. Anisotropic materials possess directionally dependent properties, meaning their mechanical and physical behaviour varies with the direction of applied forces. In this context, elastic properties such as Young's modulus, shear modulus, and Poisson's ratio differed along various axes, reflecting the anisotropic nature of the materials.

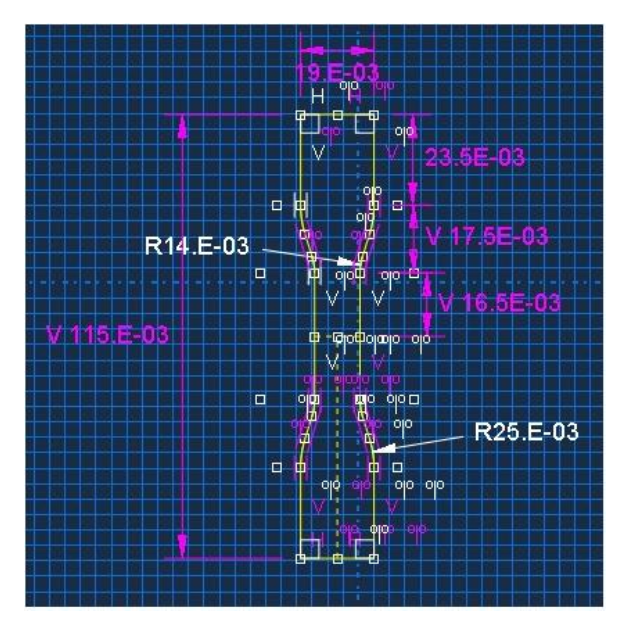


Figure 7. Sketching part

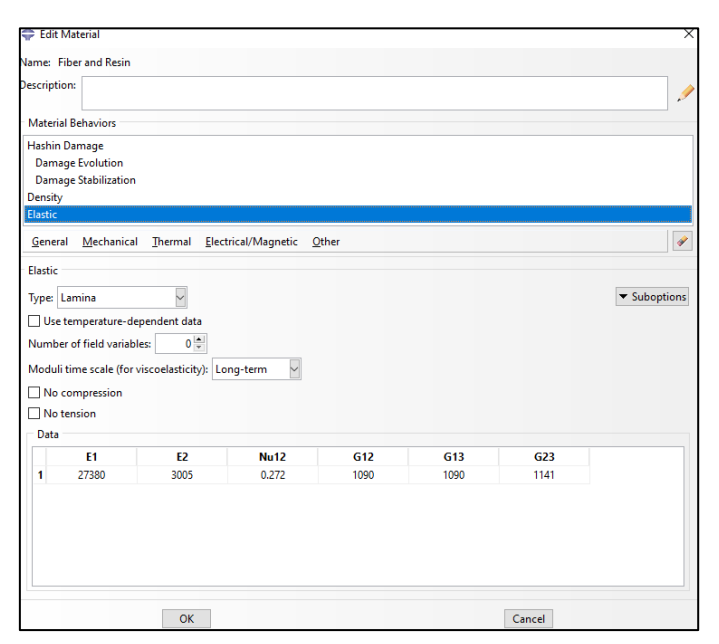


Figure 8. Lamina Property



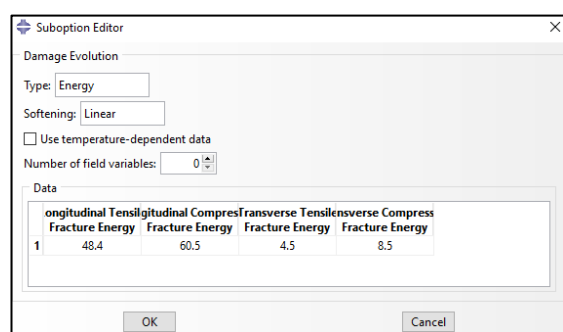
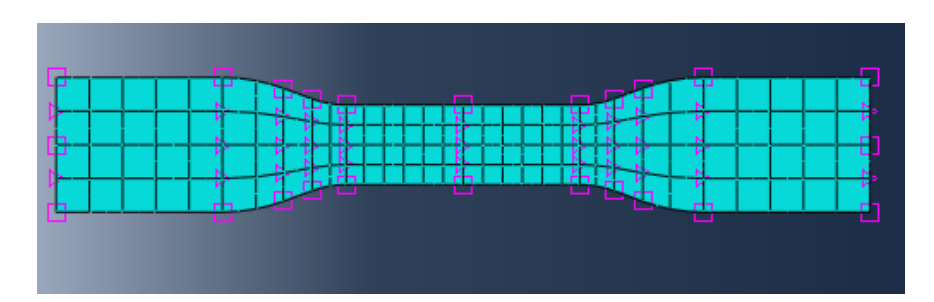


Figure 9. Hashin property

The mesh structure of the model was designed using only quadrilateral (quad) elements, specifically quad shell elements, to ensure accurate and efficient simulation results. Quadrilateral elements were chosen due to their superior performance in capturing geometry and stress distribution. As illustrated in Figure 10, the mesh was structured with five nodes along the length of the part, which is essential for accurately applying boundary conditions later in the 'Load' step. The "edge by number" process was employed to seed the top and bottom edges of the part, ensuring the creation of the correct number of elements. By selecting the top and bottom edges and specifying an even number of elements, the mesh was evenly divided, resulting in uniform element distribution. This structured mesh with five nodes along the part simplifies the application of boundary conditions, allowing for precise and consistent application of loads, constraints, and other boundary conditions, ultimately leading to more reliable simulation results.

The convergence analysis graph, as shown in Figure 11, illustrates that the load increased significantly as the number of nodes increased from 2.5 to 3.5, rising from approximately 2.7 kN to 5.3 kN. Beyond this point, the load values began to stabilize, reaching about 5.8 kN at five nodes. This trend indicates that the results have converged, as further increases in the number of nodes produce minimal changes in the load. Therefore, the model achieved convergence at five nodes, suggesting that this mesh density is sufficient to ensure accurate and reliable simulation results.

The boundary conditions (BCs) were crucial for accurately modelling the physical test by specifying the constraints and displacements on the created part to closely match the physical test conditions. Node sets were created at the top and bottom of the specimen, as illustrated in Figure 12. A displacement boundary condition was then applied to simulate the effect of a tensile force being exerted on the specimen, pulling it in the direction of the force. This setup allows for the accurate simulation of a tensile test, where the applied displacement at the top pulls the specimen, and the fixed bottom maintains stability, ensuring that the stresses, strains, and deformation patterns observed in the simulation closely match those in the actual physical test, thereby providing reliable and meaningful results. The analysis results are subsequently visualized as contour plots and graphs, which highlighted deformation patterns, stress concentration regions, and strain distribution. Finally, the discussion and conclusion focus on interpreting the results, where the simulation models are validated against experimental data. The validation confirms their accuracy and reliability, with discrepancies maintained below 9% [27].



**Figure 10.** Meshing the part with 5 nodes

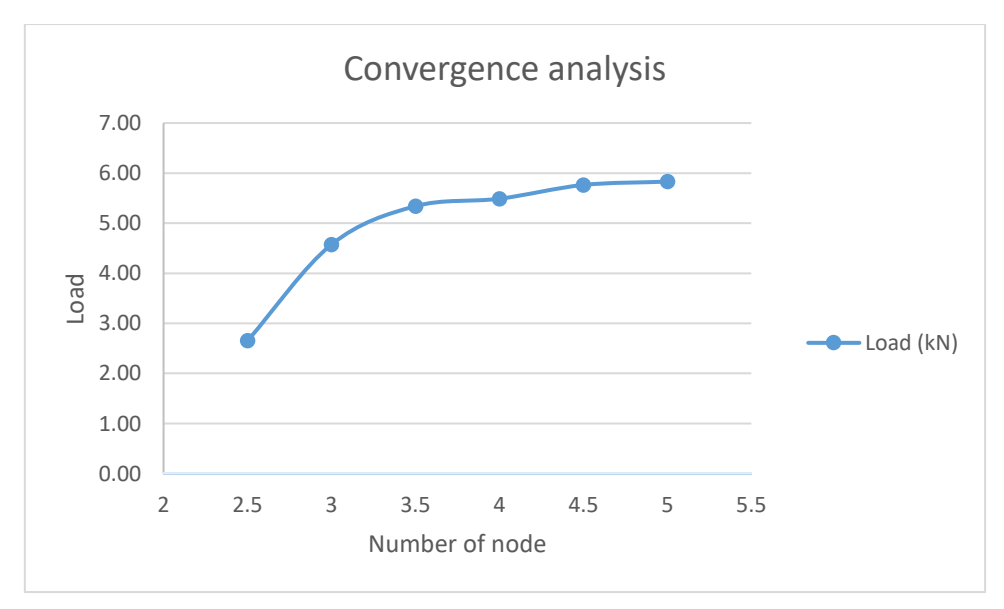


Figure 11. Convergence Analysis



Figure 12. Boundary Condition of part in Top and Bottom

#### 2.3 Fibrous structures

The fibre volume fractions of both glass fibre and banana fibre were determined using Equation 1 and Equation 2, in accordance with ASTM D2584 standards. These calculations establish the composite volume fraction by evaluating the ratio of each constituent's volume to the total volume of the hybrid composite. This step is essential for evaluating the mechanical properties and ensuring the optimal fibre-to-resin ratio in the composite material [28].

$$V_f = \left[ \rho_m \cdot w_f / \left( \rho_m \cdot w_f + \rho_f \cdot w_m \right) \right] \tag{1}$$

$$V_m = \begin{bmatrix} 1 - V_f \end{bmatrix} \tag{2}$$

where  $V_f$  volume fraction of fibres,  $w_f$  weight of fibres,  $w_m$  weight of matrix,  $\rho_f$  density of fibres,  $\rho_m$  density of matrix,  $V_m$  volume fraction of matrix.

#### 2.4 Specimen detail

**Table 1** summarizes the density and weight characteristics of glass fibre, banana fibre, and the matrix. The density of glass fibre ( $\rho_{gf}$ ) was notably high at 2.5 g/cm³, attributed to its composition, mainly 54% SiO<sub>2</sub>, 15% Al<sub>2</sub>O<sub>3</sub>, and 12% CaO, which are typical of Woven Roving reinforcement [20]. In contrast, banana fibre ( $\rho_{bf}$ ) had a lower density of approximately 1.25 g/cm³, as it is sourced solely from the pseudostem of the banana plant, the only part suitable due to the reduced strength of the other tree sections [7]. The matrix density  $\rho_m$ , made from epoxy resin, was the lowest among the three materials at about 1.175 g/cm³, owing to the specific resin compound ((CH)<sub>3</sub>C(C<sub>6</sub>H<sub>4</sub>OH)<sub>2</sub>) used in the glass-epoxy composite formulation [20]. The weight of each material of glass fibre ( $w_{mbf}$ ), banana fibre ( $w_{mbf}$ ), and the matrix was calculated per layer and applied consistently across all respective fibre layers in the specimens.

Table 2 presents the volume fractions of six different laminate configurations (L1 to L4), each consisting of varying layers of glass fibre (GF), banana fibre (BF), and matrix material. Laminate L1 was composed entirely of nine layers of glass fibre without any banana fibre. This configuration resulted in the highest total fibre weight of 9.78 grams and a relatively low matrix weight of 7.68 grams. Consequently, it yielded the highest fibre volume fraction (V<sub>f</sub>) of 36% and a matrix volume fraction (V<sub>m</sub>) of 64.1%. The high fibre density of 22.5 g/cm³ significantly contributed to the overall fibre weight, even with less matrix content. As a result, Laminate L1 exhibited the highest mechanical properties among all configurations, primarily due to its increased fibre volume fraction [29]. In contrast, Laminate L2 consisted of nine layers of banana fibre with no glass fibre. Due to the lower density of banana fibre (11.25 g/cm³), the total fibre weight was only 4.19 grams, while the matrix weight was significantly higher at 23.05 grams. This resulted in a much lower fibre volume fraction of 13.8% and a matrix volume fraction of 86.2%. The lower density of banana fibre directly reduces the fibre's weight contribution, demonstrating how both fibre density and the number of layers influence the final weight distribution [28].

Laminate L3 incorporated a hybrid composition of four layers of glass fibre and five layers of banana fibre. This arrangement produced a combined fibre density of 16 g/cm³, contributing to a total fibre weight of 6.67 grams and a matrix weight of 16.22 grams. The resulting fibre and matrix volume fractions were 20.0% and 80.0%, respectively. Laminate L4, on the other hand, consisted of five layers of glass fibre and four layers of banana fibre. This slightly increased the combined fibre density to 18 g/cm³, leading to a total fibre weight of 7.29 grams and a matrix weight of 14.51 grams. As a result, the fibre volume fraction rose to 22.1%, while the matrix volume fraction decreased to 77.9%. The increase in fibre content slightly enhanced the mechanical properties of Laminate L4 compared to L3, in line with the higher fibre volume fraction [30].

**Table 1:** Properties of Fibre and Matrix [7] [20]

Property	Value	Unit
Density Glass Fibre $(\rho_{gf})$	2.5	g/cm3
Weight of Glass Fibre $(w_{gf})$	1.086	g
Density of Banana Fibre $(\rho_{bf})$	1.250	g/cm3
Weight of Banana Fibre $(w_{bf})$	0.466	g
Density of Matrix $(\rho_m)$	1.1	g/cm3
Weight of matrix for glass fibre $(w_{mgf})$	0.854	g
Weight of matrix for banana fibre $(w_{mbf})$	2.561	g

**Table 2:** Fibre volume fraction for composite layup configurations

Laminate	Poly		Total Density (g/cm <sup>3</sup> )		Total Weight (g)		<b>Volume Friction</b>	
	GF	BF	Fibre	Matrix	Fibre	Matrix	Fibre (V <sub>f</sub> )	Matrix (V <sub>m</sub> )
L1	9	0	22.50	9.90	9.78	7.68	35.9%	64.1%
L2	0	9	11.25	9.90	4.19	23.05	13.8%	86.2%
L3	4	5	16.25	9.90	6.67	16.22	20.0%	80.0%
L4	5	4	17.50	9.90	7.29	14.51	22.1%	77.9%

#### 2.5 Material properties for simulation

These properties define the behaviour and characteristics of the composite materials under different conditions. To generate a realistic simulation model, these material properties were meticulously extracted from several credible sources. **Table 3** tabulates the properties, showing the specific values and parameters used to ensure the simulation closely replicates actual performance. By integrating these properties into the simulation, it becomes possible to predict how the composite materials will respond to various stresses and strains, thereby providing valuable insights into their tensile properties and overall mechanical behaviour.

The lamina properties for glass fibre and banana fibre were sourced from Monzón et al. [27]. The Hashin material properties for Glass Fibre + Epoxy were derived from Koloor et al. However, there is a lack of studies providing the material properties for Banana Fibre + Epoxy. Consequently, this study assumes that the Hashin properties for both Glass Fibre + Epoxy and Banana Fibre + Epoxy are identical, as referenced in Callister [31].

**Table 3.** Material properties for simulation [27] [31]

1 10 10 11 11	Property	Unit	Banana	Glass
			Fibre	Fibre
	$E_{11}$	MPa	1286.7	27380
Lamina Property	$E_{22}$	MPa	1288.8	3005
(Deepan et al.,	$V_{12}$		0.384	0.272
2023; Santhanam et	$G_{12}$	MPa	453.2	1090
al., 2020)	$G_{23}$	MPa	449.1	1090
	$G_{31}$	MPa	449.2	1141
	$X_T$	MPa	1340	820
	$X_{C}$	MPa	1192	500
	$Y_{T}$	MPa	19.6	80.6
	$Y_{C}$	MPa	92.3	322
Hashin Material	$S_{\mathrm{L}}$	MPa	51	54.5
Properties (Koloor et al., 2020)	$S_{T}$	MPa	23	161.2
,,	$G_{XT}$	N/mm	48.4	32
	$G_{XC}$	N/mm	60.5	20
	$G_{YC}$	N/mm	4.5	4.5
	$G_{YC}$	N/mm	8.5	4.5

#### 3.0 RESULTS AND DISCUSSION

### 3.1 Tensile specimen

**Figure 13** (a) to (d) shows the specimens subjected to a tensile test according to ASTM D-638. The experimental results were then validated by comparing with the simulation outcomes. The tests were conducted at a controlled rate of 1 mm/min to ensure consistent loading conditions for all specimens. The validation process started by comparing the results from the physical experiment with the simulation for each specimen. This comparison involved analysing how closely the simulated results matched the experimental data in terms of key parameters for tensile property. Any discrepancies between the two sets of results were examined to identify possible reasons, such as differences in material properties, boundary conditions, or assumptions made in the simulation model.

When comparing the experimental specimens for configurations L1 (**Figure 13** (a)), L3 (**Figure 13** (c)) and L4 (**Figure 13** (d)), it was observed that even though the tensile test reached the maximum tensile load, the specimens did not completely fracture. Instead, they developed cracks, primarily because the stress was uniformly distributed across the middle section of the specimens [27].

The analysis of simulated specimens with a higher proportion of glass fibre compared to banana fibre, such as L1 (shown in **Figure 13** (a)), L3 (shown in **Figure 13** (c)) and L4 (shown in **Figure 13** (d)), revealed that the highest stress values were concentrated in the middle section of each specimen, likely where the cross-sectional area was smallest. This was indicated by the colour scale, with red representing the highest stress and blue the lowest. Such stress concentration is typical in tensile tests and highlights potential failure points under tensile loading. The colour scale exhibited a linear gradient from the centre towards the ends of the specimens, suggesting they were subjected to a uniform tensile load. This resulted in a consistent variation in stress along the length, with a uniform stress distribution across the cross-section at any given point, indicating that the tensile test was accurately simulated with evenly applied loads. Similar simulations pattern was observed in Monzón et al. as the stress was concentrated in the middle zone.

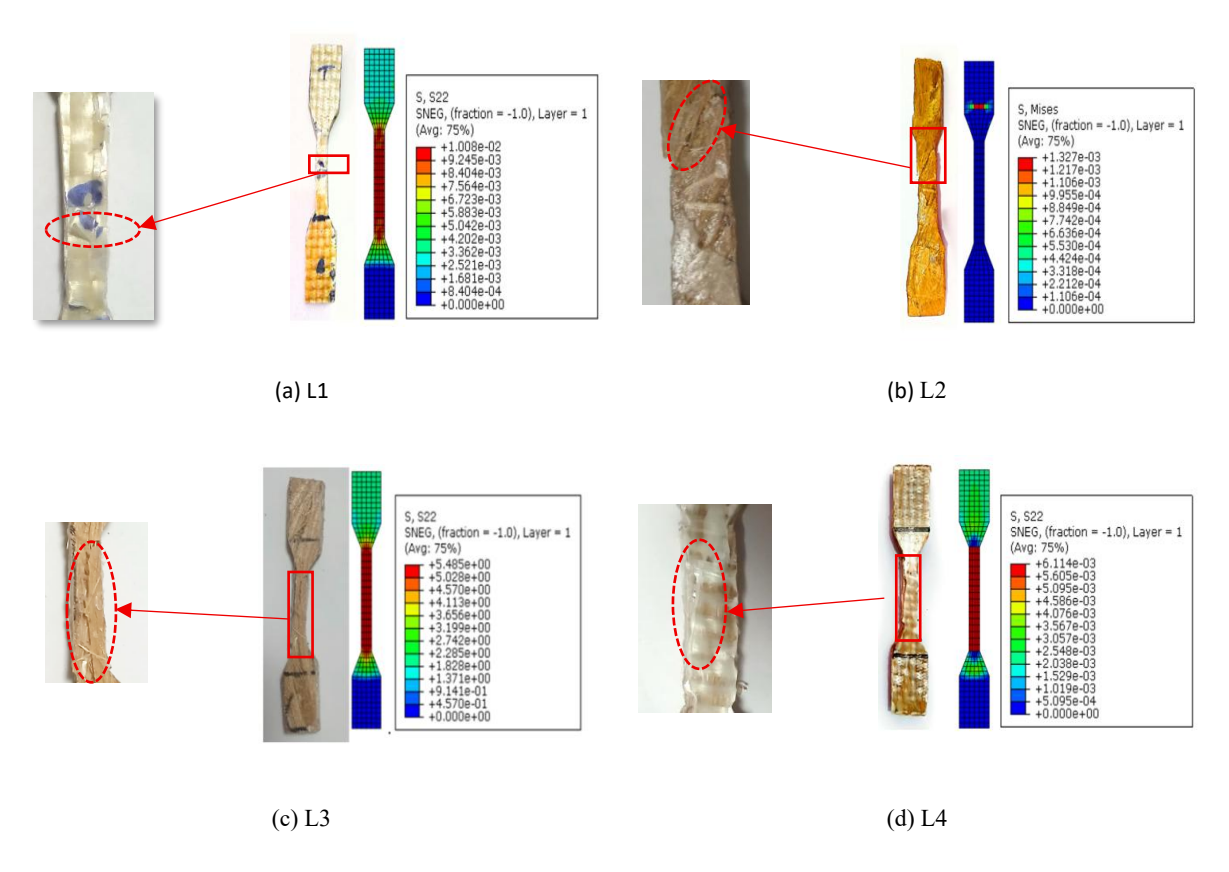


Figure 13. Tensile test specimen after the experiment and simulation

In experimental L2, as depicted in Error! Reference source not found. (b), this stress distribution pattern I ed to the formation of a crack, particularly at the top middle, indicating that the specimen was on the verge of failure at this location[27], [32]. This partial damage reflects the uneven distribution of stress and the material's varying resistance across different regions. The banana fibres outnumbered glass fibres as the stress distribution showed a distinct pattern. The contour plot stress decreased from the centre toward the edges, a phenomenon rooted in the distinct mechanical properties of the fibres. Glass fibres, known for their superior strength and stiffness, bear a larger portion of the load, resulting in higher stress concentrations in the central region of the specimen. As the load is transferred outward towards the edges, where banana fibres are more prevalent, the stress diminishes. This is due to banana fibres being less stiff and less strong, making them less effective at resisting the applied load. The adhesion loss between the fibres and the matrix leads to the initiation of fibre breakage and pull-out [8]. Consequently, the material exhibits a stress gradient, with higher stress levels at the centre and lower levels at the edges—a characteristic common in uniformly loaded composite materials, where stronger materials are positioned to handle more stress in the central regions, and weaker materials manage less stress towards the periphery.

#### 3.2 Comparison of the composition configuration

**Table 4** tabulates the comparison between the experiment and the simulation results. The simulation results for the 9-glass fibre (GF) plies showed a slight overestimation of both peak load and ultimate stress compared to the experimental values. In Experiment L1, the ultimate load recorded was 5.96 kN, while the simulation predicted 5.83 kN, showing a small difference of 2.18%. The ultimate stress from the experiment was 119.46 MPa, slightly higher than the simulation's 119.06 MPa, with a 0.33% difference. For Experiment L2, the ultimate load measured was 1.13 kN, while the simulation showed 1.11 kN, a difference of 1.77%. The ultimate stress recorded was 10.17 MPa, compared to the simulation's 9.84 MPa, resulting in a 3.24% difference. In Experiment L3, the ultimate load was 3.72 kN, and the simulation predicted 3.78 kN, showing a 1.61% difference. The ultimate stress recorded was 36.57 MPa, slightly lower than the simulation's 36.77 MPa, with a 0.55% difference. Lastly, for Experiment L4, the ultimate load measured was 4.23 kN, while the simulation gave 4.17 kN, with a difference of 1.42%. The ultimate stress in the experiment was 52.46 MPa, while the simulation showed 52.08 MPa, resulting in a 0.73% difference.

For all four (4) types of materials, the simulated values for both peak load and ultimate stress are generally close to the experimental values, as indicated by the low percentage errors. The percentage errors are relatively small, suggesting that the simulation results are in good agreement with the experimental data. Overall, the simulation seems to be performing well in predicting the mechanical behaviour of the tested methods, with the differences between experimental and simulated values being within reasonable limits.

 Table 4: Comparison between experiment and simulation results

Sample	Method	Peak Load (kN)	Ultimate Stress (MPa)	
т 1	Experiment	5.96	119.46	
L1 9 plies GF	Simulation	5.83	119.06	
9 piles Gr	Percentage error	2.18	0.33	
1.0	Experiment	1.13	10.17	
L2	Simulation	1.11	9.84	
9 plies BF	Percentage error	1.77	3.24	
L3 5 plies BF + 4	Experiment	3.72	36.57	
	Simulation	3.78	36.77	
plies GF	Percentage error	1.61	0.55	
L4	Experiment	4.23	52.46	
4 plies BF + 5	Simulation	4.17	52.08	
plies GF	Percentage error	1.42	0.73	

# 3.3 Load displacement and stress strain curves

Figure 14 presents the experimental and simulation results of Load versus Displacement for L1. Initially, both curves exhibited a linear increase as the applied load increased, continuing this trend until reaching their respective peak loads. The experimental results showed a peak load of 5.96 kN at a displacement of 6.42 mm, while the simulation results indicated a maximum load of 5.83 kN at 7.45 mm. These peak values represent the material's maximum load capacity, signifying the complete failure of the matrix material in the laminate. The remaining portion of the graph illustrates the progressive failure of the reinforcing material [33].

This result is essential for verifying whether the experimental outcome meets the required specifications based on the selected method. To ensure accuracy, the experimental result was compared with the data from Stanciu et al. [34], which reported a value of 5.738 kN. The calculated percentage error was approximately 3.83%. Additionally, the comparison between the experimental and simulation results revealed a close alignment in both load-displacement. The discrepancies were minimal, with only a 2.18% variation in ultimate load (kN), where the experiment yielded 5.96 kN and the simulation produced 5.83 kN.

Figure 15 presents the stress-strain curve for L1, comparing experimental and simulation results to provide key insights into its tensile behaviour. Initially, the curve follows a linear trend at low strain values. This linearity persists until the material reaches its ultimate tensile strength. The peak stress, representing the ultimate tensile strength, was recorded at 119.46 MPa with a strain of 10.94% in the experiment and 119.06 MPa with a strain of 13.55% in the simulation. This corresponded to a 0.33% variation in ultimate stress between the experimental and simulation results. Furthermore, the obtained values align with the reported range of ultimate stress from previous studies, such as 120 MPa by Prem Chand et al. [35] and 228 MPa by Stanciu et al. [34], confirming that the results fall within an acceptable range.

The graph in Figure 16 illustrates the relationship between load and displacement, comparing experimental data with simulation data for L2. Both the experimental and simulation curves exhibited an upward trend, indicating that as displacement increased, the load required also increased [23]. In the initial phase, both curves exhibited a relatively steep slope. In the mid-region, the curves became less steep, with the experimental curve reached 1.13 kN at a displacement of 4.02 mm, while the other curve attained 1.11 kN at a displacement of 3.42 mm. Towards the final stage, the curves gradually flattened out. The peak load values are considered acceptable, as they fall within the acceptable range based on previous references [23] [27] [3].

Moreover, the experimental and simulation curves showed some similarities, but there were noticeable differences. The simulation curve generally lies above the experimental curve, indicating that the simulation predicts slightly higher load for a given displacement compared to the actual experiment [36]. The ultimate load recorded in the experiment was 1.13 kN, while the simulation predicted an ultimate load of 1.11 kN. This comparison indicates that the results for load displacement are closely aligned, with only a slight discrepancy of 1.77% in the ultimate load (kN).



Figure 14. Load vs Displacement curve for L1

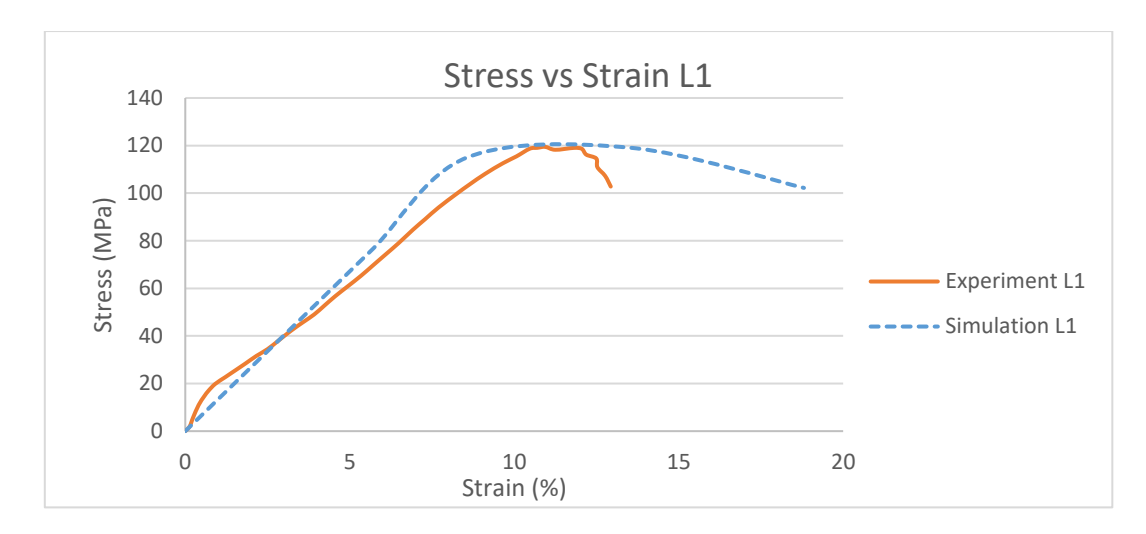


Figure 15. Stress vs strain curve for L1



Figure 16. Load vs displacement curve for L2

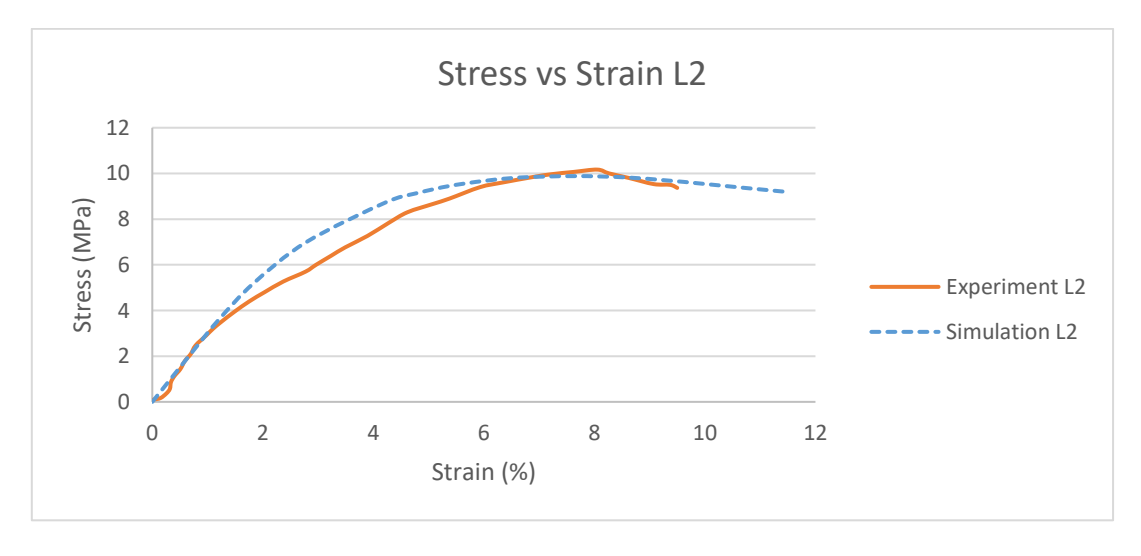


Figure 17. Stress vs strain curve for L2

Figure 17 illustrates a comparison of the stress-strain behaviour observed in Experiment L2 and Simulation L2, revealing several key differences between the two datasets. Both curves demonstrated an increase in stress as strain increased. However, Simulation L2 initially exhibited a steeper slope in comparison to Experiment L2 [36]. In terms of peak stress and strain, Simulation L2 reached a maximum stress of approximately 9.84 MPa at a strain of 6.82%, while Experiment L2 achieved a higher peak stress of 10.17 MPa at a strain of 8.05%. These results are deemed acceptable as they align with the expected range outlined in previous references [23][37].

The ultimate stress recorded in experiment L2 was 10.17 MPa, whereas simulation L2 predicted an ultimate stress of 9.84 MPa. This comparison highlighted that the results for stress-strain were closely aligned, with only a slight discrepancy of 3.24% in the Ultimate Stress. This minor difference underscores a generally good agreement between the experimental and simulated results, despite the observed variations. Additionally, the comparison between glass fibre and banana fibre reveals that while both materials exhibit similar trends, banana fibre has lower mechanical properties than glass fibre [38]

The graph in Figure 18 presents Load versus Displacement for L3 which compares experimental and simulated data, illustrating the relationship between load and displacement. At the initial stage, both curves originated from the zero point and in the mid-region, the experimental curve exhibited a steeper slope compared to the simulation [36], reaching a maximum load of 3.72 kN at a displacement of 6.92 mm, whereas the simulation recorded a maximum load of 3.78 kN at a displacement of 6.85 mm.

As a result, the ultimate load recorded in the experiment was 3.72 kN, while the simulation predicted a slightly higher ultimate load of 3.78 kN. The material failure in the laminate during the tensile test is attributed to fibre pull-out in the composite [35]. This comparison indicates a close agreement between the experimental and simulation load-displacement results, with only a minor discrepancy of 1.61% in the ultimate load.

Figure 19 presents a line graph showing the experimental and simulation Stress versus Strain curves for L3. Both the experimental and simulation curves followed a similar trend. Initially, stress increased almost linearly with strain, showing similar elastic behaviour. The ultimate stress reached at 36.57 MPa with a strain of 11.27% in the experiment, while in the simulation, it occurred at 36.77 MPa with a strain of 11.42%.

Both graphs on Load vs. Displacement and Stress-Strain curves reveal a noticeable discrepancy in the slopes between the experimental and simulation results. This deviation arises due to factors such as void formation, uneven fibre distribution, and potential delamination of layers inherent in the hand layup technique. The FEA by used the ABAQUS software effectively captures the material's linear elastic behaviour across various stacking sequences. However, more advanced simulations are required to accurately model the plastic behaviour of composites, particularly for fatigue-related applications [36].

The maximum stress, or strength, observed in the experiment was slightly higher than the simulation's prediction. For instance, the ultimate stress in experiment L3 was recorded at 36.57 MPa, compared to the 36.77 MPa predicted by simulation L3. This comparison reveals that the load displacement and stress-strain results are very close, with only a minimal difference of 0.55% in ultimate stress.



Figure 18. Load vs displacement curve for L3

Figure 20 presents the Load versus Displacement results, where the experimental load graphs exhibited a general trend of increasing load and stress with displacement, progressing through distinct phases before reaching their peak values. Initially, L3 followed a linear upward trend until they reached the maximum load stress [37]. The experimental results peaked at 4.23 kN at a displacement of 5.45 mm, while the simulation reached a slightly lower peak of 4.17 kN at 5.0 mm. Notably, after reaching the peak, the experimental data showed a load drop to 3.20 kN at 5.32 mm, whereas the simulation did not exhibit this immediate drop but instead gradually decreased to 3.61 kN at 7.80 mm. The comparison simulation and experiment of ultimate load shows a close match in the load-displacement results, with only a slight deviation of 1.42% in ultimate load (kN).

Figure 21 illustrates the Stress versus Strain relationship, where both the experimental and simulated results followed a similar trend. The experimental peak stress was recorded at 52.46 MPa at 8.95% strain, while the simulation reached 52.08 MPa at 8.47% strain. Additionally, the ultimate stress in experiment L3 was recorded at 52.46 MPa, closely matching the 52.08 MPa predicted by simulation L4. The stress-strain results align closely, with just a minimal difference of 0.73% of simulation and experiment.

Both graphs are similar to L3, which reveal a clear difference in slopes between the simulation and experiment, attributed to voids, uneven fibre distribution, and potential layer delamination in the hand layup process. While Abaqus effectively predicts the material's linear elastic behaviour, more advanced simulations are required to model plastic behaviour, particularly for fatigue applications [36].

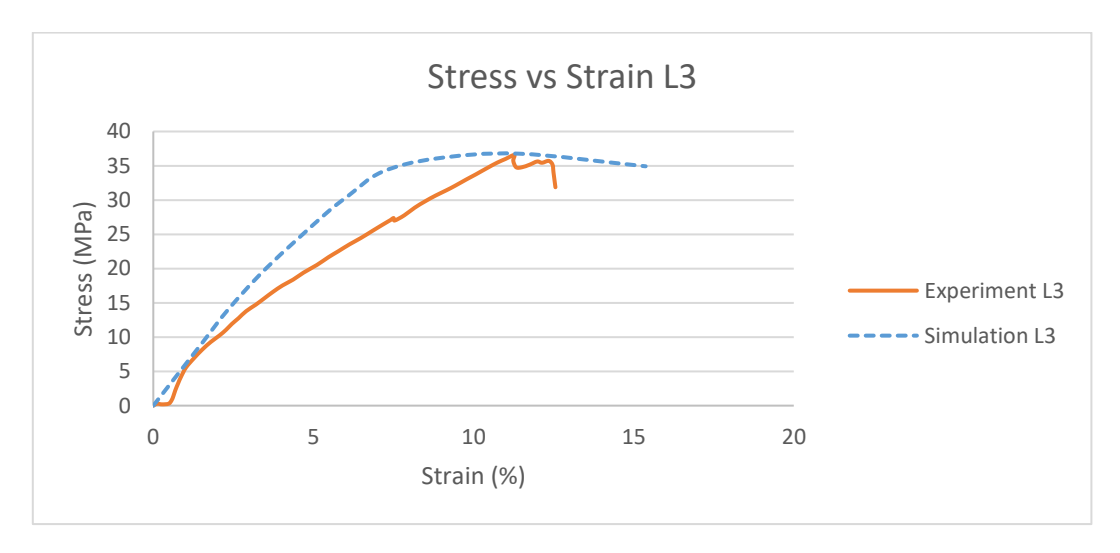


Figure 19. Simulation stress vs strain curve for L3

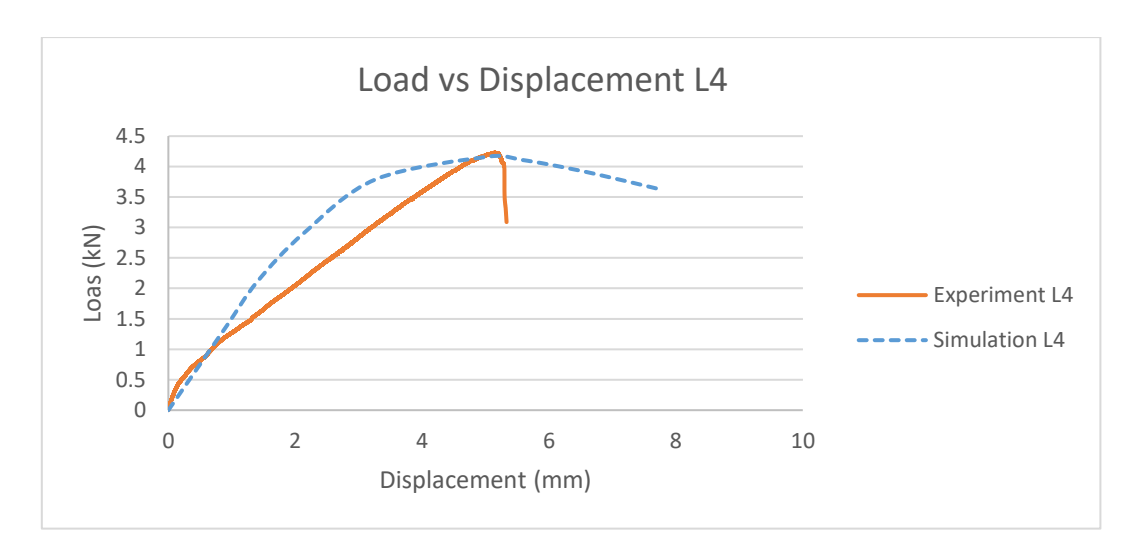


Figure 20. Load vs displacement curve for L4

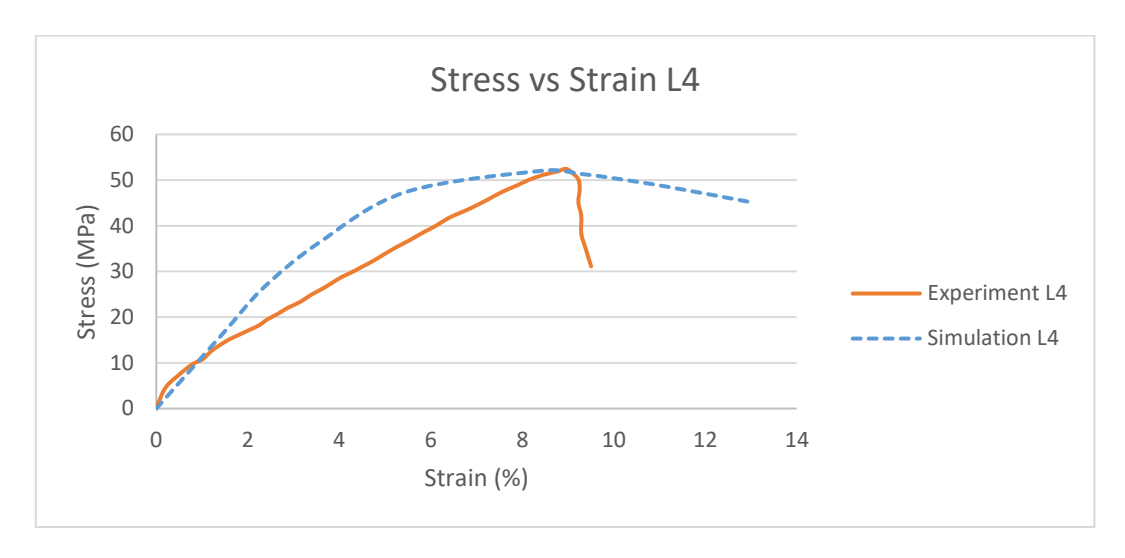


Figure 21. Stress vs strain curve for L4

# 4.0 CONCLUSION

The first objective of this study was to determine the optimal tensile properties of glass fibre and banana fibre composites in various configurations by modifying their layer arrangements. This objective was successfully achieved. The tensile performance of the composite materials was optimized by altering the stacking sequence of glass and banana fibre layers. Among all configurations, L1, composed entirely of glass fibre, exhibited the highest tensile strength, achieving a peak load of 5.96 kN and an ultimate stress of 119.46 kN. The L4 configuration, consisting of five plies of glass fibre and four plies of banana fibre, recorded a peak load of 4.23 kN and an ultimate stress of 52.46 kN. Similarly, L3, which contained four plies of glass fibre and five plies of banana fibre, demonstrated a peak load of 3.72 kN and an ultimate stress of 36.57 kN. Finally, L2, made entirely of nine plies of banana fibre without glass fibre reinforcement, exhibited the lowest tensile properties, with a peak load of 1.13 kN and an ultimate stress of 10.17 kN.

The second objective, which aimed to validate the tensile properties obtained from simulation results against experimental findings, was also successfully accomplished. The validation confirmed that the simulation model accurately predicted the tensile behaviour of the composite materials, demonstrating strong agreement between experimental and simulated results and reinforcing the model's reliability. The specimens were modelled using finite element analysis (FEA) in Abaqus, and a detailed comparison between experimental and simulation data provided valuable insights into the mechanical behaviour of epoxy composites reinforced with glass and banana fibres. The load—displacement and stress—strain curves consistently highlighted the superior strength of glass fibre compared to banana fibre, as observed in both experimental and simulated outcomes. The comparison revealed an average percentage error of 9% between the peak load (kN) and ultimate stress (MPa). Specifically, the errors for peak load and ultimate stress were 2.18% and 0.33% for L1, 1.77% and 3.24% for L2, 1.61% and 0.55% for L3, and 1.42% and 0.73% for L4, respectively.

# **ACKNOWLEDGEMENT**

This project is funded by the FRGS/1/2002/TK0/UITM/02/60 and Universiti Teknologi MARA under FRGS scheme: 600-RMC/FRGS 5/3(077/2022). The authors also would like to thank Universiti Teknologi MARA, Cawangan Pulau Pinang for the management support.

#### **AUTHORS CONTRIBUTION**

Mustafa Nordin: Formal analysis, investigation, Methodology, Writing-Original Draft

Mohd Rozaiman Aziz: Supervision, Conceptualization, Methodology, Validation, Writing-Review & Editing,

Resources

Rozaini Othman: Supervision, Conceptualization, Methodology, Validation, Writing-Review& Editing

# **DECLARATION OF COMPETING OF INTEREST**

The authors declare that they have no known competing financial interests or personal relationships that could have appeared to influence the work reported in this paper.

#### **REFERENCES**

- [1] M. Ismail, M. R. M. Rejab, J. P. Siregar, Z. Mohamad, M. Quanjin, and A. A. Mohammed, "Mechanical properties of hybrid glass fiber/rice husk reinforced polymer composite," *Mater Today Proc*, vol. 27, no. April, pp. 1749–1755, 2020, doi: 10.1016/j.matpr.2020.03.660.
- [2] H. Pranoto and M. Fitri, "The Effect of Alkali Treatment to Mechanical Properties of Resin Composite Reinforced with Coir Coconut Fiber," 2022.
- [3] B. Sampath, N. Naveenkumar, P. Sampathkumar, P. Silambarasan, A. Venkadesh, and M. Sakthivel, "Experimental comparative study of banana fiber composite with glass fiber composite material using Taguchi method," in *Materials Today: Proceedings*, Elsevier Ltd, 2021, pp. 1475–1480. doi: 10.1016/j.matpr.2021.07.232.
- [4] M. Yahiya and N. Venu Kumar, "A review on natural fiber composite with banana as reinforcement," *Mater Today Proc*, 2023, doi: 10.1016/j.matpr.2023.03.211.
- [5] Y. V. Ravi, N. Kapilan, S. Rajole, Y. S. Balaji, N. Varun Kumar Reddy, and B. K. Venkatesha, "Damage resistance evaluation of E-glass and hybrid hemp-banana natural fiber composite helmet using drop weight impact test," *Mater Today Proc*, vol. 54, pp. 330–335, Jan. 2022, doi: 10.1016/j.matpr.2021.09.213.
- [6] R. Prem Chand, B. S. Halemani, K. M. Chandrasekhar, Y. P. Ravitej, T. Hemanth Raju, and S. Udayshankar, "Investigation and analysis for mechanical properties of banana and e glass fiber reinforced hybrid epoxy composites," in *Materials Today: Proceedings*, Elsevier Ltd, 2021, pp. 2509–2515. doi: 10.1016/j.matpr.2021.05.044.
- [7] L. Prabhu *et al.*, "Experimental investigation on mechanical properties of flax/banana/ industrial waste tea leaf fiber reinforced hybrid polymer composites," in *Materials Today: Proceedings*, Elsevier Ltd, 2021, pp. 8136–8143. doi: 10.1016/j.matpr.2021.02.111.
- [8] M. V. K. Reddy, R. V. S. Lakshmi, Y. Pragathi, P. Devaraj, and N. Naresh, "Evaluation of mechanical properties: Influence of glass fiber on banana fiber reinforced with epoxy composite," in *Materials Today: Proceedings*, Elsevier Ltd, 2020, pp. 1305–1312. doi: 10.1016/j.matpr.2020.06.467.
- [9] R. Karthick, K. Adithya, C. Hariharaprasath, and V. Abhishek, "Evaluation of mechanical behavior of banana fibre reinforced hybrid epoxy composites," 2018. [Online]. Available: www.sciencedirect.comwww.materialstoday.com/proceedings2214-7853
- [10] R. Pai, L. Bangarappa, K. S. Lokesh, D. Shrinivasa Mayya, C. R. Naveen, and T. Pinto, "Hybridization effect on water absorption and flexural properties of E-glass/banana fibre/epoxy composites," in *Materials Today: Proceedings*, Elsevier Ltd, 2022, pp. 1841–1845. doi: 10.1016/j.matpr.2021.11.491.
- [11] S. Thangaraj, A. Ranjith kumar, M. Vigneshwaran, M. Muthuraj, R. Shenbagaraj, and R. Girimurugan, "Distinctive study on banana/sisal fiber hybrid composites filled with nano marble dust particles," *Mater Today Proc*, 2023, doi: 10.1016/j.matpr.2023.01.402.
- [12] S. Deepan, R. Jeyakumar, V. Mohankumar, and A. Manojkumar, "Influence of rice husk fillers on mechanical properties of banana/epoxy natural fiber hybrid composites," in *Materials Today: Proceedings*, Elsevier Ltd, Jan. 2023, pp. 575–580. doi: 10.1016/j.matpr.2022.09.459.
- [13] Md. M. H. Kanok, S. S. Shifa, M. S. Haque, and A. Akter, "Comparative study on mechanical properties of banana-glass fiber reinforced epoxy hybrid composites," *Mater Today Proc*, Sep. 2023, doi: 10.1016/j.matpr.2023.08.356.
- [14] V. Santhanam, R. Dhanaraj, M. Chandrasekaran, N. Venkateshwaran, and S. Baskar, "Experimental investigation on the mechanical properties of woven hybrid fiber reinforced epoxy composite," in *Materials Today: Proceedings*, Elsevier Ltd, 2020, pp. 1850–1853. doi: 10.1016/j.matpr.2020.07.444.
- [15] T. Batu and H. G. Lemu, "Investigation of mechanical properties of false banana/glass fiber reinforced hybrid composite materials," *Results in Materials*, vol. 8, Dec. 2020, doi: 10.1016/j.rinma.2020.100152.
- [16] T. A. Negawo, Y. Polat, Y. Akgul, A. Kilic, and M. Jawaid, "Mechanical and dynamic mechanical thermal properties of ensete fiber/woven glass fiber fabric hybrid composites," *Compos Struct*, vol. 259, Mar. 2021, doi: 10.1016/j.compstruct.2020.113221.
- [17] S. Omprakasam, P. Vishnu, B. M. Ishanna, S. Abinaya Sree, and R. Divya Rani, "Banana fiber with madar fiber composites for sustainable printed circuit boards," *Mater Lett*, vol. 380, Feb. 2025, doi: 10.1016/j.matlet.2024.137750.
- [18] S. S. R. Koloor, A. Karimzadeh, N. Yidris, M. Petrů, M. R. Ayatollahi, and M. N. Tamin, "An energy-based concept for yielding of multidirectional FRP composite structures using a mesoscale lamina damage model," *Polymers (Basel)*, vol. 12, no. 1, 2020, doi: 10.3390/polym12010157.
- [19] A. Al Rashid, M. Y. Khalid, R. Imran, U. Ali, and M. Koc, "Utilization of banana fiber-reinforced hybrid composites in the sports industry," *Materials*, vol. 13, no. 14, 2020, doi: 10.3390/ma13143167.
- [20] S. K. Kotla Rachana, "DEVELOPMENT AND TESTING OF GLASS FIBRE REINFORCED COMPOSITES," 2020. [Online]. Available: http://www.ijeast.com

- [21] K. Jubair, M. S. Islam, and D. Chakraborty, "Investigation of Mechanical Properties of Banana-Glass Fiber Reinforced Hybrid Composites," *Journal of Engineering Advancements*, pp. 175–179, Nov. 2021, doi: 10.38032/jea.2021.04.002.
- [22] T. Seshaiah, K. Vijaya, and K. Reddy, "EFFECT OF FIBER ORIENTATION ON THE MECHANICAL BEHAVIOR OF E-GLASS FIBRE REINFORCED EPOXY COMPOSITE MATERIALS." [Online]. Available: www.tjprc.org
- [23] M. R. Sanjay, G. R. Arpitha, L. Laxmana Naik, K. Gopalakrishna, and B. Yogesha, "Studies on mechanical properties of Banana/E-Glass fabrics reinforced polyester hybrid composites," *Journal of Materials and Environmental Science*, vol. 7, no. 9, pp. 3179–3192, 2016.
- [24] S. Shankar, H. K. Shivanand, and E. P. Koorapati, "Comparative Study of Experimental and Simulated Results of Compression Test on Epoxy Based E-Glass / Carbon Fiber Reinforced Polymer Composite Laminates," *International Journal of Emerging Technology and Advanced Engineering*, vol. 4, no. 8, pp. 288–296, 2014.
- [25] M. D. Monzón *et al.*, "Experimental analysis and simulation of novel technical textile reinforced composite of banana fibre," *Materials*, vol. 12, no. 7, pp. 1–23, 2019, doi: 10.3390/ma12071134.
- [26] Abaqus, "ABAQUS VERSION 6.6 DOCUMENTATION," Abaqus. [Online]. Available: https://classes.engineering.wustl.edu/2009/spring/mase5513/abaqus/docs/v6.6/books/exa/default.htm?st artat=ch01s04aex50.html
- [27] M. D. Monzón *et al.*, "Experimental analysis and simulation of novel technical textile reinforced composite of banana fibre," *Materials*, vol. 12, no. 7, pp. 1–23, 2019, doi: 10.3390/ma12071134.
- [28] M. El Messiry, "Theoretical analysis of natural fiber volume fraction of reinforced composites," *Alexandria Engineering Journal*, vol. 52, no. 3, pp. 301–306, 2013, doi: 10.1016/j.aej.2013.01.006.
- [29] "An\_Investigation\_into\_the\_Effects\_of\_Fibre\_Volume\_Fraction\_on\_GFRP\_Plate\_1.pdf".
- [30] L. Ciprian, P. Radu, and E. Ioana, "The Effects of Fibre Volume Fraction on a Glass-Epoxy Composite Material," *INCAS BULLETIN*, vol. 7, no. 3, pp. 113–119, Sep. 2015, doi: 10.13111/2066-8201.2015.7.3.10.
- [31] J. William D. Callister, *Material Science And Engineering An Introduction*, Sixth Edit. United States of America, 2003.
- [32] H. Xin, Y. Liu, A. S. Mosallam, J. He, and A. Du, "Evaluation on material behaviors of pultruded glass fiber reinforced polymer (GFRP) laminates," *Compos Struct*, vol. 182, pp. 283–300, 2017, doi: 10.1016/j.compstruct.2017.09.006.
- [33] R. Prem Chand *et al.*, "Characterization of banana and e glass fiber reinforced hybrid epoxy composites," in *Materials Today: Proceedings*, Elsevier Ltd, 2021, pp. 9119–9125. doi: 10.1016/j.matpr.2021.05.402.
- [34] M. D. Stanciu, H. T. Drăghicescu, and I. C. Roșca, "Mechanical properties of GFRPs exposed to tensile, compression and tensile—tensile cyclic tests," *Polymers (Basel)*, vol. 13, no. 6, Mar. 2021, doi: 10.3390/polym13060898.
- [35] R. Prem Chand *et al.*, "Characterization of banana and e glass fiber reinforced hybrid epoxy composites," in *Materials Today: Proceedings*, Elsevier Ltd, 2021, pp. 9119–9125. doi: 10.1016/j.matpr.2021.05.402.
- [36] A. Al Rashid, M. Y. Khalid, R. Imran, U. Ali, and M. Koc, "Utilization of banana fiber-reinforced hybrid composites in the sports industry," *Materials*, vol. 13, no. 14, Jul. 2020, doi: 10.3390/ma13143167.
- [37] M. K. Moon, S. Saha, A. Biswas, and A. A. Paul, "Characteristics and Comparative Study of Sodium Hydroxide Treated Banana Fiber Reinforced Composite Material," *IOP Conf Ser Mater Sci Eng*, vol. 1305, no. 1, p. 012029, Apr. 2024, doi: 10.1088/1757-899x/1305/1/012029.
- [38] L. Karthick, S. Sivakumar, A. Sasikumar, A. Prabhu, J. Senthil Kumar, and L. Vadivukarasi, "A comparison and analysis of mechanical properties of glass fiber and banana fiber composite," in *Materials Today: Proceedings*, Elsevier Ltd, 2022, pp. 398–402. doi: 10.1016/j.matpr.2021.09.073.